Multiple-Model Control Strategy of a Fed-Batch High Cell-Density Culture Process

Yu-Cheng Chung[1], I-Lung Chien[1] and Der-Ming Chang[2,*]

1. Department of Chemical Engineering, National Taiwan University of Science and Technology, Taipei 106, Taiwan, R.O.C.
2. Department of Bioindustry Technology, Da Yeh University, Changhua 515, Taiwan, R.O.C.

Abstract

The fermentation of microorganisms is an important practice in the biotechnology industry. To enhance the volumetric productivity, high cell concentration and high cell productivity are required. Owing to the inherent feature of cell growth, an exponential feeding profile is practiced. However, exponential feeding needs sophisticated control techniques. Moreover, for aerobic high cell-density culture (HCDC) processes, when the amounts of biomass and of bio-products increase in the fermenter, the rate of oxygen mass transfer and the dissolve oxygen will decrease. Therefore, the specific growth rate of microorganism will descend slowly. Due to the substrates (carbon and oxygen) simultaneously influence the growth rate of microorganisms, a good operating methodology in HCDC processes must maintain the concentrations of those substrates. The object in this work is to construct a simple but robust control strategy for this specific process. Through the system analysis, the new control methodology is proposed. The overall control structure includes an optimal feedforword controller and a multiloop SISO feedback controller. Moreover, in the feedback loops, multiple-models are used such that the proposed control structure is very simple to build. The scheduled controllers for each loop tuned by Internal Model Control (IMC) principle were proposed. The novel control structure was shown by simulation that not only performs better than Generic Model Control (GMC) but also has robust properties to the mismatch in the model's form. The productivity of the proposed strategy is 37.5% more than the GMC's in the simulation.

1. Introduction

The fermentation of microorganisms for producing biomass, primary and secondary metabolites, proteins, and other biopolymers are an important practice in the biotechnology industry. Hence, the primary goal of fermentation research is the cost-effective production of bio-products. To enhance the volumetric productivity, high cell concentration and high cell productivity are required, where this operation is usually achieved through fed-batch cultivation [1,2]. Owing to the inherent feature of cell growth, an exponential feeding profile has been proven to be the most usable technique to maintain growth rates in biomass in industry [3,4,5]. However, exponential feeding needs sophisticated control techniques. The common difficulty in these

open-loop strategies is that no compensation is made for modeling errors or random disturbances arising in the process operation [6,7]. Since both overfeeding and underfeeding of nutrient is detrimental to cell growth and product formation, development of a suitable control strategy is critical in fed-batch cultivation. Therefore, from another viewpoint, interest has subsequently moved to the design of controller configurations that will make the system follow an optimum trajectory calculated off-line [6].

In recent years, several robust adaptive controllers were designed to track the product trajectory in a fed-batch fermenter in which the kinetics are complex and most of the state variables are difficult to measure [8,9]. However, these methods need knowledge of the full states of the studied systems. For most bioprocesses in which there is a deficiency of reliable on-line sensors, an extended Kalman filter is used to estimate states and parameters. Briefly, these methods have complex control structure and hence are not usually convenient to be used in a real plant. For this reason, the simple indirect feedback control schemes that couple nutrient feeding with measurement of pH (pH-stat) or DO (DO-stat) have been developed [2,10]. On the other hand, the expert system based on fuzzy control or neural networks has developed and holds promise for optimizing fed-batch techniques for complex fermentation systems [11,12]. Although these simple or advanced methods have several advantages, the suboptimal productivity or unstable system has arisen frequently.

Moreover, in the fermentation processes of high cell-density culture (HCDC), another critical problem is the lack of oxygen uptake. When the amounts of biomass and/or of bio-products increase in the fermenter, the rate of oxygen mass transfer and dissolve oxygen will decrease; therefore, the specific growth rate of microorganism will descend slowly [1,2]. In this case, the toxic components may produce, e.g., acetate when *E. coli* is grown under anaerobic or oxygen-limiting condition [2]. Therefore, the dynamic behavior of this kind of process has a result of accumulation of the substrates the same as the multiple-substrate processes [7]. The accumulating action continually recurs. This behavior, similar to the snowball effect in plant-wide control, will let the process run away [7,13]. Consequently, a good control methodology for HCDC processes must be able to maintain the concentrations of two substrates, i.e., carbon and oxygen, simultaneously.

In this work, the fed-batch HCDC process will be described as a multivariable system. Through the system analysis, a new control strategy is proposed. This strategy is to combine an optimal feedforward controller (**FFC**) and a multiple SISO feedback controller (**FBC**). To schedule this time-varying process, multiple-model approach is used to describe the process such that the proposed control methodology is very simple to build. Finally, the performance of the overall control strategy will be shown via simulation.

2. Modeling, Optimal Operating, and Characteristics of the Process

There are many important physical variables, e.g., temperature, pH, and concentration of the inhibitors, in HCDC process. In this work, we assumed most variables, i.e., temperature, pH, etc., are under controlled for simplicity. Therefore, the dynamics of the process can be analyzed in detail.

Process Modeling The fermentation processes that carried out by fed-batch-operating method was considered. Except carbon source, the dissolved oxygen is also a limited-substrate for an aerobic culture of microorganism in HCDC. In a well-mixed bioreactor, these can be modeled by the following set of governing equations [13,14] as:

$$(\dot{XV}) = \mu XV \tag{1}$$

$$(\dot{SV}) = -\sigma XV + S_F u \tag{2}$$

$$(\dot{C_{DO}V}) = [\mathrm{OTR} - \mathrm{OUR}]V \tag{3}$$

$$\dot{V} = u \tag{4}$$

where X, S, and C_{DO} are the concentration of cell, carbon and oxygen source in broth, respectively. V is the working volume, u stands for the inlet volumetric flow rate, and S_F is the feed substrate concentration. Considering both carbon and oxygen source as essential substrates and the deterministic and non-structured mathematical model of the specific growth rate (μ) in HCDC fermentation process is used. If the carbon source is with inhibition at high concentration of

substrate, the μ can be described as

$$\mu = \mu_{\max}\left(\frac{S}{K_S + S + S^2/K_I}\right)\left(\frac{C_{DO}}{K_O + C_{DO}}\right) \quad (5)$$

where $\mu_{\max}$ is the maximum specific growth rate and K_S and K_I are parameters in the inhibition growth kinetic model for carbon source, and K_O is the parameter in the Monod model of oxygen source. The specific growth rate like Eq. (5) was called Haldane-Monod model in this work.

The specific carbon source consumption rate (σ) is:

$$\sigma = \frac{\mu}{Y_{SX}} \quad (6)$$

where Y_{SX} is the yield coefficient from carbon source to cell. For oxygen source, the oxygen transfer rate (OTR) and oxygen uptake rate (OUR) are given as:

$$\text{OTR} = k_L a\left(HC_{O2} - C_{DO}\right) \quad (7)$$

$$\text{OUR} = \left(\mu / Y_{OX}\right) X \quad (8)$$

where k_La and Y_{OX} are the overall mass transfer of the oxygen and the yield coefficient from oxygen source to cell, respectively. C_{O2} is the mole fraction of the gaseous oxygen in the fermenter. H is a parameter related to Henry's law constant for oxygen in water. The relationship between k_La and the agitation speed (Γ) is assumed to be:

$$K_L a = \alpha\left(\Gamma\right)^{\beta} \quad (9)$$

where α, β are constants. Due to that oxygen was supplied from gas phase, we must have another equation to describe oxygen balance. From the mass balance of the oxygen in gaseous phase, the rate of accumulation of the gaseous oxygen is:

$$\left(\dot{C}_{O2}V\right) = \frac{RT}{\varepsilon PM}\left[-\text{OTR}V + \frac{PMQ}{RT}\left(y_{in} - C_{O2}\right)\right] \quad (10)$$

where y_{in} is the oxygen mole fraction of the inlet air, R is universal gas constant. T and P are the temperature and pressure in the bioreactor, respectively. In addition, M and Q stand the molecular weight of oxygen and the flow rate of inlet air, respectively, and ε denotes the fraction of the reactor that is occupied by the gas phase.

Optimal (Feedforward) operation The operating criterion of a fermentation process is to obtain the maximum bio-products. In fed-batch culture, the objective here is to determine the feed rate profile $u(t)$ that maximizes the cell production rate:

$$\max_u \quad J = \frac{X(t_f)V(t_f) - X(t_0)V(t_0)}{t_f} \quad (11)$$

where t is the fermentation time and subscripts 0 and f denote the initial and final conditions, respectively. The feed profile crosses the singular arc segment, i.e., the more interesting exponential feeding, depends on

$$u^* = X^* V^* \left(\frac{\sigma^*}{S_F - S^*}\right) \quad (12)$$

where superscript * describes the optimal value of the state. In inhibition growth kinetic model, the optimal concentration of the carbon source is $S^* = \sqrt{K_S K_I}$ [5]. Substituting Eq. (12) into Eq. (2), the time derivative of the optimal S^* becomes zero. This means that the exponential feeding policy will maintain the concentration of carbon source in the fermenter. Owing to the fact that the dissolve oxygen for the cell growth rate is Monod kinetic model, the cell growth rate of the process approximately reaches to the maximum value only if the concentration of the dissolve oxygen is greater than several folds of K_O. Consequently, the optimal dissolved oxygen, C_{DO}^*, is conservatively set at ten folds of K_O in this work.

For holding the concentration of the dissolved oxygen, similar to carbon source, we can analyze from the steady-state of the system. Therefore, after rearranging Eqs. (3) and (10), we obtain:

$$\dot{C}_{DO} = -C_{DO}\frac{u}{V} + [\text{OTR} - \text{OUR}] \quad (13)$$

and

$$\dot{C}_{O2} = \frac{RT}{\varepsilon PM}\left[-\frac{\varepsilon PM}{RT}\frac{u}{V}C_{O2} - \text{OTR} + \frac{PMQ}{RTV}\left(y_{in} - C_{O2}\right)\right] \quad (14)$$

Since we want to hold C_{O2} and C_{DO} at constant values, the left-hand side of Eqs. (13) and (14) will become zero. Furthermore, after applying the optimal feed as in Eq. (12) and the OTR and OUR as in Eqs. (7) and (8), we obtain the following relationships as:

$$k_L a = \frac{\frac{C_{DO}^* \sigma^*}{S_F - S^*} + \frac{\mu^*}{Y_{OX}}}{HC_{O2}^* - C_{DO}^*} X^* \quad (15)$$

and

$$\left(y_{in}-C_{O2}^{*}\right)Q=\left[\frac{RT}{PM}\left(\frac{C_{DO}^{*}\sigma^{*}}{S_F-S^{*}}+\frac{\mu^{*}}{Y_{OX}}\right)+\frac{\varepsilon C_{O2}^{*}\sigma^{*}}{S_F-S^{*}}\right]X^{*}V^{*} \tag{16}$$

Eqs. (15) and (16) show that k_La is proportional to X^* and $\left(y_{in}-C_{O2}^{*}\right)Q$ is proportional to X^*V^*. In a general case, the speed of the agitator is used for regulating C_{DO}. Therefore, from the Eq. (16) and Eq. (9), the speed of regulator is

$$\Gamma^{*}=\left(\frac{(K_La)^{*}}{(K_La)_0}\right)^{-\beta}\Gamma_0=\left(\frac{X^{*}}{X_0}\right)^{-\beta}\Gamma_0 \tag{17}$$

Hereafter, the subscript 0 describes the initial value of the variable. Furthermore, choosing $Q^{*}=\left(V^{*}/V_0\right)Q_0$, from Eq. (16), we can use y_{in} to maintain C_{O2} as

$$y_{in}^{*}=\frac{X^{*}}{X_0}\left(y_{in,0}-C_{O2,0}^{*}\right)+C_{O2}^{*} \tag{18}$$

In this section, a optimal feedforward operating strategy is built for the HCDC process. This feedforward operating strategy, which notated as **FFC**, will obtain the maximum productivity of cell in a nominal plant. For implementation, S, C_{DO} and C_{O2} are maintained at optimum values by u^*, Γ^*, and y_{in}^{*} in above Eqs. (12), (17), and (18). A schematic of **FFC** is shown in Figure 1.

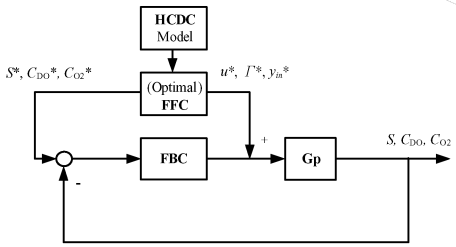

Figure 1. *Schematic diagram of the proposed control strategy.*

Characteristics of the Process Dynamic Base on the above discussion, a optimal **FFC** controller is constructed for fed-batch HCDC process. However, in the real world, a plant generally has various types of uncertainties. For this, the snowball effect can be arisen [7] which may cause the process to run away. In this section, we will show this phenomenon by simulations. Table 1 lists the parameters and initial values of a typical fed-batch HCDC process. Figure 2 displays the simulation results when there exist 20% mismatch in the model parameters. The figure with the dynamic responses for the positive and negtive mismatches are not symmetric because the system has snowball effect. The snowball effect occurs when the corbon source is accumulated due to mismatch in the model parameter [7]. Table 2 summaries the directions which existing the snowball effect for each model parameter. Based on above discussion, a worst uncertain case that combinded all cases to have the snowball effect with error in model's paremeters can be built.

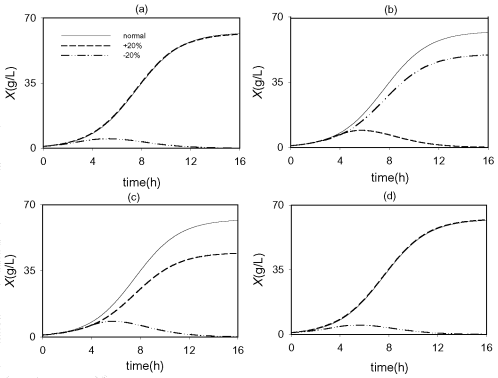

Figure 2. *Responses of the plant with* ***FFC*** *for mismatch in model parameter (a)* μ_{max}*, (b)* Y_{XS}*, (c)* Y_{OS}*, and (d)* α *&* β*.*

Table 1 *Parameters and initial conditions of an aerobic fed-batch fermentation process.*

Parameters			
μ_{max} (h^{-1})	1.132	K_S (g/L)	0.4606
K_O (g/L)	0.0001	K_I (g/L)	1.8537
Y_{OX} (--)	2.0	Y_{SX} (--)	0.7
P (atm)	1.9	T (K)	310
M (g/mol)	32	H (g/L)	0.0663
α (1/h)(rpm) $^{-\beta}$	10	β (--)	0.5
ε (--)	0.15		
Initial Conditions			
S_F (g/L)	90.0	X_0 (g/L)	1.0
S_0 (g/L)	1.0	V_0 (m^3)	0.2
$(C_{DO})_0$ (ppm)	1.0	$(C_{O2})_0$ (--)	0.19
Q_0 (L/h)	1142.6	Γ_0 (rpm)	14.8

Table 2 *Summary of the snowball effect with the mismatch in various model parameters.*

	Positive deviation	Negative deviation
μ_{max}		+
Y_{SX}	+	
Y_{OX}		+
α, β		+
u	+	

+: with snowball effect

Figure 3 (a) shows the dynamic response of the process in this worst case. Oppositely, if combined all errors in the model's paremeters that don't cause the snowball effect, the dynamic response of process will not exhibit run away behavior. In addition, for common uncertainties in fermentation processes, the mismatch in feed rate measurement and oxygen-limited cases are also shown in Figure 3 (b) and (c), respectively. The snowball effects again occurred only in one direction. Therefore, we will use three worst cases to test the performance of the proposed control structure in the following section.

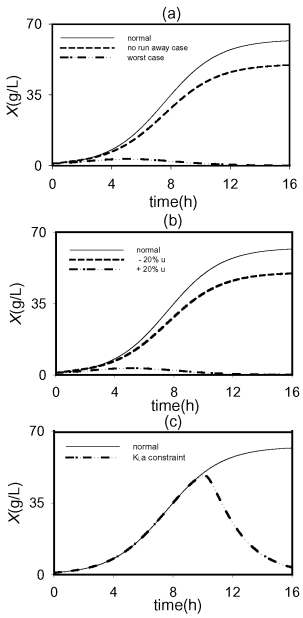

Figure 3. *Responses by simulation for (a) the worst case with combination of several model parameter mismatches, (b) the feed-rate error, and (b) the oxygen-limited case.*

3. Feedback Controller Design

In the above section, the characteristics of the dynamic in the fed-batch HCDC process were discussed. The key point in HCDC process is that the snowball effect is arisen only if there are oxygen-limited or carbon-overloaded situation. Therefore, the HCDC process is displayed as a multivariable system to simultaneously considering the carbon and oxygen sources. In this section, we will discuss a novel feedback control strategy to avoid the above snowball problem. This proposed strategy (i.e., **FBC**) is based on the process that included with the optimal feedforward operating policy (**FFC**) (see Figure 1).

System Analysis To design the feedback control system, the process with the optimal feedforward control was considered. Therefore, the system can be linearized around its optimal value [7]. The linearlized process can be displayed as a state-spaced linear system as

$$\begin{bmatrix} \dot{X} \\ \dot{S} \\ \dot{C}_{DO} \\ \dot{C}_{O2} \\ \dot{V} \end{bmatrix} = \begin{bmatrix} -\left(\frac{u^*}{V^*}-\mu^*\right) & 0 & \mu^*\left(\frac{X^*}{C^*_{DO}}\right)\left(\frac{K_O}{K_O+C^*_{DO}}\right) & 0 & \frac{X^*u^*}{V^{*2}} \\ -\sigma^* & -\frac{u^*}{V^*}-\sigma^*\left(\frac{X^*}{C^*_{DO}}\right)\left(\frac{K_O}{K_O+C^*_{DO}}\right) & 0 & -\frac{u^*}{V^{*2}}\left(S_F-S^*\right) & \\ -\frac{\mu^*}{Y_{OX}} & 0 & -a_1 & H(K_La)^* & \frac{u^*C^*_{DO}}{V^{*2}} \\ 0 & 0 & \frac{RTK_La^*}{\varepsilon PM} & -a_2 & \frac{u^*C^*_{O2}}{V^{*2}} \\ 0 & 0 & 0 & 0 & 0 \end{bmatrix} \begin{bmatrix} X \\ S \\ C_{DO} \\ C_{O2} \\ V \end{bmatrix} + \begin{bmatrix} -\frac{X^*}{V^*} & 0 & 0 \\ \frac{S_F-S^*}{V^*} & 0 & 0 \\ -\frac{C^*_{DO}}{V^*} & \alpha\beta\left(HC^*_{O2}-C^*_{DO}\right)\Gamma^{*(\beta-1)} & 0 \\ -\frac{C^*_{O2}}{V^*} & -\frac{\alpha\beta\left(HC^*_{O2}-C^*_{DO}\right)}{\varepsilon PM}\Gamma^{*(\beta-1)} & \frac{Q_0}{\varepsilon V_0} \\ 1 & 0 & 0 \end{bmatrix} \begin{bmatrix} u \\ \Gamma \\ y_{in} \end{bmatrix} \quad (19)$$

where

$$a_1 = \left[K_La^* + \frac{u^*}{V^*} + \left(\frac{\mu^*X^*}{Y_{OX}C^*_{DO}}\right)\left(\frac{K_O}{K_O+C^*_{DO}}\right)\right] \quad (20)$$

and

$$a_2 = \left[\frac{HRT\left(K_La\right)^*}{\varepsilon PM} + \frac{u^*}{V^*} + \frac{Q_0}{\varepsilon V_0}\right] \quad (21)$$

Eq. (19) explains that the plant is a high-order system and its denominator should be 5th-order. Because the role of the feedback control is to compensate uncertainty within the fed-batch process, the feedback controller is to reject the disturbance mainly at high frequency. Therefore, the DRGA analysis [15] was used to analyze the pairing of control loops as

$$\mathbf{\Lambda}\Big|_{s=j\omega} = \left(\mathbf{G}_P\Big|_{s=j\omega}\right) \otimes \left(\mathbf{G}_P\Big|_{s=j\omega}^{-1}\right)^T \qquad (22)$$

where $\mathbf{G}_p(s) = \mathbf{C}(s\mathbf{I}-\mathbf{A})^{-1}\mathbf{B}$; **A**, **B** are obtained from Eq. (19) and **C** = [0 1 0 0 0; 0 0 1 0 0;0 0 0 1 0] assuming S, C_{DO}, and C_{O2} are measurable. Moreover, the parameters of system are time-varying. They are function of the optimal values and the several constants of system. The state X^* has a point of inflection (see Figure 2). From analyzing $X^*(t)$, we know that this event takes place at

$$t_{IF} = \frac{\ln\left[X_\infty^{\,2}\left(\frac{X_\infty^* - X_0}{X_\infty^* X_0}\right)^2\right]}{2\mu^*} \qquad (23)$$

where X_∞^* is concentration of biomass at infinite time for the optimal fermentation condition. The plant changes its dynamic characteristics at this point (discussed in detail at later). The diagonal DRGAs are displayed in Figure 4. The figure shows that the recommended pairing of the system decoupled at high frequency for the initial, inflecting point, and final time of the process. The recommended pairing is to control S by manipulating u, C_{DO} by manipulating Γ, and C_{O2} by manipulating y_{in}.

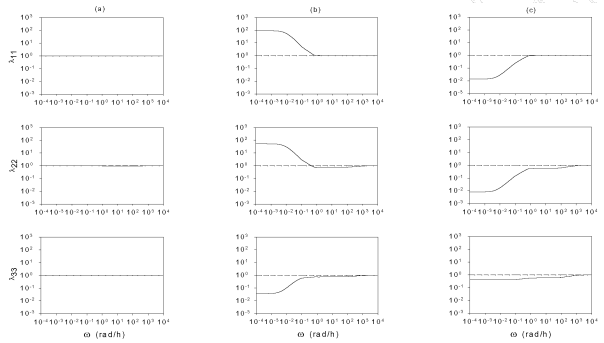

Figure 4. *Diagonal of DRGA for HCDC process at (a) initial time, (b) inflecting point, and (c) final time.*

Building Multiple-Model From above analysis, the control structure is determined, i.e., a multiloop SISO control system is used. Moreover, the transfer functions for each loop are shown to be higher order and time-varying. It is impractical to design three high order controllers and then use them in industry. Therefore, the goal is to design the controllers as simple as possible. In order to obtain a simpler model,

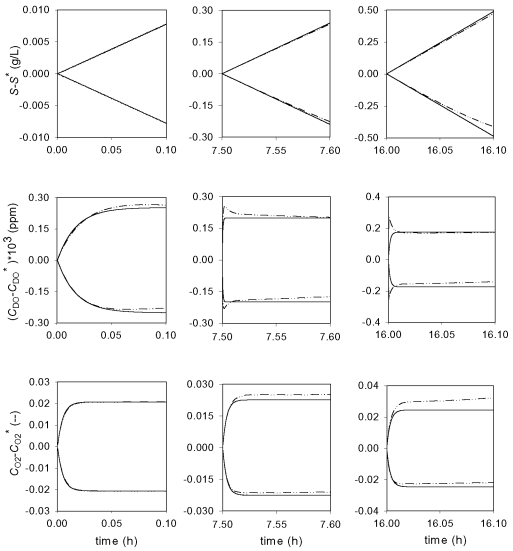

Figure 5. *Open-loop responses at three critical times: (a) initial, (b) inflecting point, and (c) final.*

an off-line identification method is used next. Step change response data is obtained by simulating the process model with the inclusion of the **FFC** operation. These open-loop responses at three critical times are shown in Figure 5. The dynamical characteristics are changed at inflection point in the DO loop. However, from the responses in this figure, two model types,

$$G_{M_1}(s) = \frac{k_{P_1}}{s} \qquad (24)$$

and

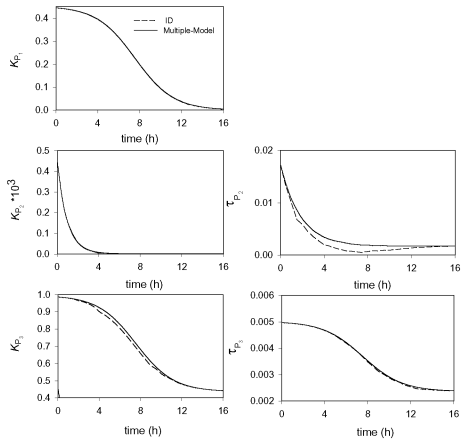

Figure 6. *Variation of the transfer functions parameters vs. time.*

$$G_{M_i}(s)=\frac{k_{P_i}}{\tau_{P_i}s+1} \qquad i=2,3 \tag{25}$$

can be used to described the dynamic responses of the carbon source (i.e., loop 1) and oxygen source (i.e., loops 2 and 3), respectively. Moreover, the parameters in the transfer functions are varied with time. Dotted lines in Fig. 6 display the changes of the parameters with time in the transfer functions in Eqs. (24) and (25). Furthermore, owing to the fact that X^* is proportional to u^*/V^* from Eq. (12), and then from the model parameter in Eq. (19), we can found out that most of the parameters in the transfer functions are changed with the optimal state X^*. Therefore, we will use X^* to build the multiple-model. Similar to gain scheduling, the model-parameter scheduling is defined by using different process models as the operating condition changes. Takagi-Sugeno method [16,17] offers a general framework to establish a nonlinear (global) model between the scheduling variable ϕ (e.g., the optimal biomass X^* or its high order form) and the scheduled variable z (e.g., steady-state gain or time constants), that is

$$z = f(\phi) \tag{26}$$

Moreover, a linear combination between two linear functions [17] is used to simplify the above expression to:

$$z = \underline{z}(1-\psi)+\bar{z}\psi \tag{27}$$

where $\bar{z}$ and $\underline{z}$ are defined as the value of scheduled variable at the upper and lower bounds of the regime, and defined Ψ as:

$$\psi = \frac{\phi-\underline{\phi}}{\bar{\phi}-\underline{\phi}} \tag{28}$$

where Ψ as a linear membership function for ϕ with $\bar{\phi}$ and $\underline{\phi}$ as the value of scheduling variable at the upper and lower bounds of the regime.

Table 3 *The identified models for the Haldane-Monod process to combine into multiple-model.*

	Initial (t = 0 h)	Final (t = 16 h)
Loop 1	$G_{M_1}=\frac{0.445}{s}$	$G_{M_1}=\frac{0.00452}{s}$
Loop 2	$G_{M_2}=\frac{4.55\times10^{-4}}{0.01728s+1}$	$G_{M_2}=\frac{8.278\times10^{-8}}{0.00168s+1}$
Loop 3	$G_{M_3}=\frac{0.9858}{0.00497s+1}$	$G_{M_3}=\frac{0.442}{0.00239s+1}$

The scheduling variable ϕ must be decided in order to complete this modeling approach. Eqs. (27) and (28) display a linear relationship between z and ϕ is described such that a suitable scheduling variable, ϕ, must be found. Figure 7 shows the pairs of the scheduling and the scheduled variables that conform to Eq. (27) (i.e., the dash lines in Figure 7). Therefore, X^* (denote as ϕ_1) is chosen to model the carbon source loop (loop 1) and gas phase loop (loop 3). However, the gain and the time constant for the transfer function of loop 2 must be $(X^*)^{-2}$ and $(X^*)^{-1}$ (denote as ϕ_{-2} and ϕ_{-1}), respectively. Although Figure 7 displays the nonlinearity in several parameters of the transfer functions, all multiple models are set up in one fuzzy implication for simplicity. The multiple-model is built by linear models at the initial and final time as seen in Table 3. The solid lines in Figure 6 display the built multiple-model. In all the three approximated models, the deviations of parameters in the transfer functions are all within tolerant limit (Figure 6).

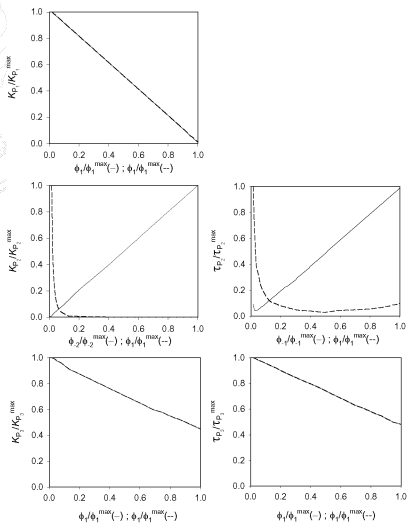

Figure 7. *Analysis for choosing the scheduling variables for multiple-model.*

Tuning of the Feedback Controllers An important item in designing the control strategy is controller tuning. The primary objective of feedback control in HCDC process is to regulate the mistakes in model parameters. Therefore, the tuning criterion is to reject this specific kind of disturbance. When the feedforward controller is applied with some model mismatches, it is

similar as a ramped load disturbance going into the system from system inputs. Since the system itself is modeled as a integrating or first-order system, the combined effect at the system output is a Type III system for loop 1 and a Type II' system for loop 2 and 3. In other word, the load for loop 1 (an integrating system) at system output is with the form:

$$d = \frac{1}{s^3} \tag{29}$$

and for loops 2, 3 (first-order systems), the load at system output is with the form:

$$d = \frac{1}{s^2\left(\tau_{p_i} s + 1\right)}, \quad i = 2,3 \tag{30}$$

The controller to reject these types of load disturbances will be constructed. First, based on final value theorem, the PI^{2}D type is necessary to rejection these kinds of load disturbances. There are three parameters need to be tuned. Moreover, owing to the fact that all model parameters of the process are changed with time, the tuning rules must be based on these parameters such that the scheduled control strategy can be carried out. For these reasons, the methodology of internal model control (IMC) was used to tune the feedback controllers [18]. The tuning rules of the feedback controller are listed in Table 4. The transfer functions of the closed-loops for loops 1~3 are:

$$G_{CL_1} = \frac{3\tau_{CL_1} s^2 + 3\tau_{CL_1} s + 1}{\left(\tau_{CL_1} s + 1\right)^3} \tag{31}$$

and

$$G_{CL_i} = \frac{2\tau_{CL_i} s + 1}{\left(\tau_{CL_i} s + 1\right)^2}, \quad i = 2,3 \tag{32}$$

Before doing some closed-loop simulation, let's summarize the procedure for the proposed control strategy as follows:

S1. obtain the coefficients to construct the process model (Eqs. (1)-(10)).

S2. set up the optimal feedforward controller (Eqs. (12), (17), and (18)).

S3. obtain the simplified linear transfer functions at the initial and final time via model identification based on model forms in Eqs. (24) and (25), and then, combined into multiple-model according to Eqs. (27) and (28).

S4. set up the PI^{2}D feedback controllers with tuning rules in Table 4.

Table 4 *Tuning rules for IMC-PI^{2}D controller.*

	k_C	τ_I	τ_D
Type II'	$\frac{\tau_P + 2\tau_{CL}}{2\tau_{CL} k_P}$	$\tau_P + 2\tau_{CL}$	$\frac{2\tau_{CL}\tau_P}{\tau_I}$
Type III	$\frac{\tau_I}{k_P \tau_{CL}^3}$	$3\tau_{CL}$	τ_{CL}

where τ_{CL} denotes the time constant of the closed-loop

S5. operate the fed-batch culture by **FFC** and **FBC**.

Closed-loop Simulation In the last section, procedure for the proposed control strategy is described. In this section, we will demonstrate the performance of the proposed control strategy with the same example shown before. A GMC controller [19] is also set up for comparison purpose. The closed-loop transfer functions of GMC are designed to be:

$$\frac{y}{y^{SP}} = \frac{2\tau\zeta s + 1}{\tau^2 s^2 + 2\tau\zeta s + 1} \tag{33}$$

The time constants of closed-loop in GMC are chosen to be 0.15 hr, 0.01 hr and 0.01 hr for loops of the carbon source, the dissolved oxygen and the oxygen in gas phase, respectively. The values of damping coefficient for each loop are set to be unity. The closed-loop time constants (τ_{CL_i}) for the purposed control strategy are set to have equal closed-loop speed of response to the GMC's. The three τ_{CL_i} are set to be 0.1 hr, 0.01 hr and 0.01 hr, respectively, for these three loops in the proposed IMC-PI^{2}D controllers. Notice that since closed-loop of loop 1 for the proposed control structure is third-order while the GMC is second-order, thus, 0.l hr is selected for the loop 1 of the proposed control structure and 0.15 hr is selected for the GMC.

Several measurement lags and measurement noise are added to each loop to simulate the dynamics with real measurement devices. These include a double first order lag with 0.005 hr time constant in the carbon loop, two first order lags with 0.001 hr time constant in the dissolved oxygen loop and also in the gas phase oxygen loop. Besides the measurement lags, two Gauss distributed noises are added in the measurement of DO (full scale of 0~2 ppm with 5% noise standard deviation) and measurement of exhaust gas (full scale of 0~100%

with 2% noise standard deviation). The simulation results with feed-rate error are shown in Figure 8. The deviation of state S in the proposed control structure is smaller than the GMC's. The trajectories of the states of the proposed control strategy are similar to the performance of the GMC. However, from Figure 9, the proposed control strategy gives better control performance for the worst case condition (i.e., combining of several mismatches in the model parameters all together). The amount of product loss is up to 37.5% by GMC strategy in comparison with the case when all the model parameters are correctly known. However, the product loss of the proposed strategy is only at 0.093%. Moreover, an upper limit in K_La is assumed to compare the compensating effect of oxygen transfer in the proposed and the GMC controllers. Although the proposed control strategy reaches to oxygen-limiting earlier, the performance of the overall response is better than the GMC's. This simulation result is demonstrates in Figure 10. However, in the oxygen-limiting case, the amount of product loss is also up to 4.84% for our proposed strategy.

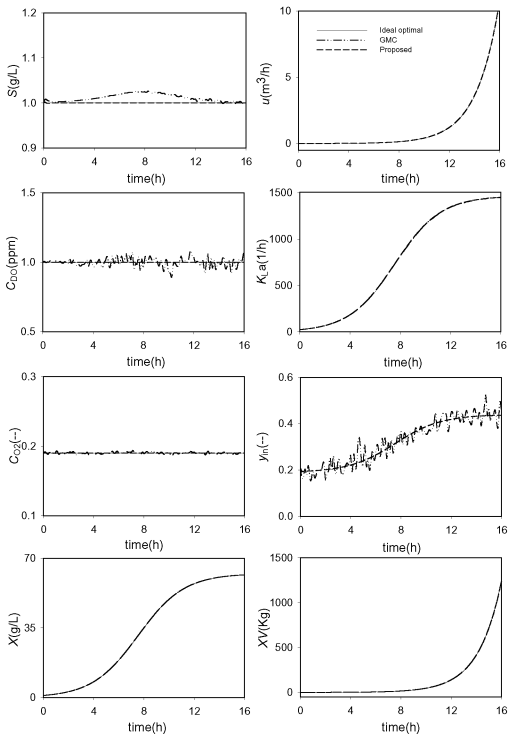

Figure 8. *State trajectories by different control strategies for feed-rate error.*

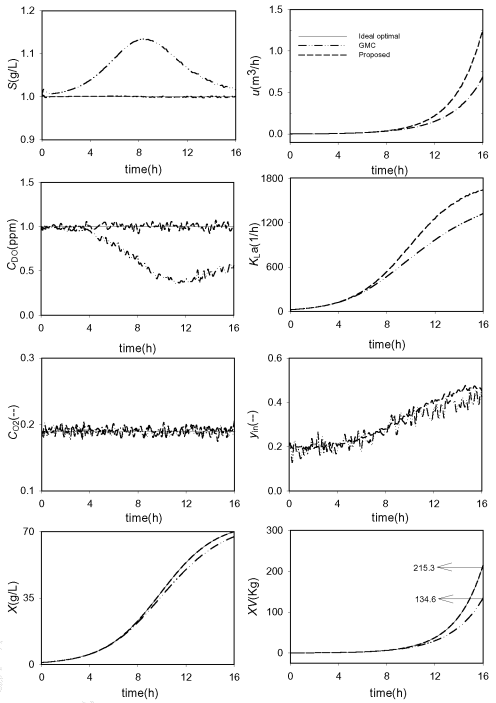

Figure 9. *State trajectories by different control strategies for model parameter mismatches.*

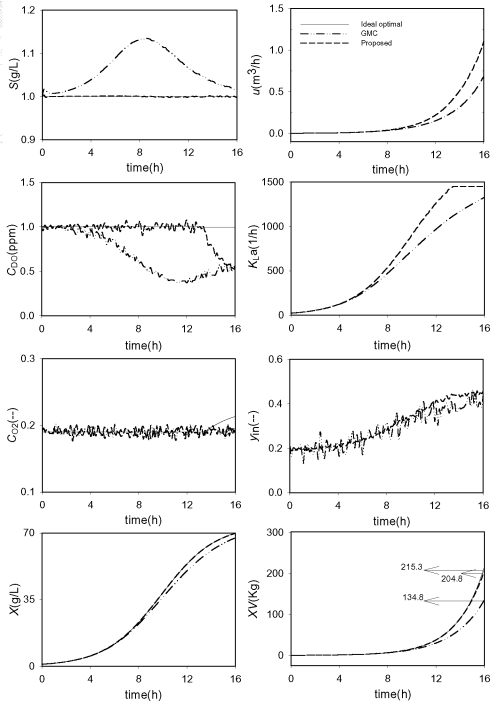

Figure 10. *State trajectories by different control strategies for model parameter mismatches in combination with oxygen-limiting.*

4. Conclusion

In this investigation, the control strategy for an important bioprocess (HCDC process) is studied. Although, our object is to build a simple but robust methodology, the process considered as a multivariable system is necessary due to two essential substrates influencing the process simultaneously. An optimal feedforward controller (**FFC**) is built first, and then through the system analysis, the new control strategy for the feedback control loops is proposed. The overall control strategy is to combine an optimal feedforword controller with a multiloop SISO feedback controller. Since each feedback loop is nonlinear and time-varying, multiple-model by fuzzy rule is used such that the proposed control structure is very simple to build and implement. The scheduled feedback controller for each loop is tuned using IMC principle. In order to reject load disturbance from model mismatches, a PI^2D feedback controller form is designed. Through closed-loop simulation, this novel control structure is shown to be not only performed better than GMC's but also robust enough to the mismatches in the model parameters as well as the model's form. The production rate of the proposed control strategy is over 37.5% than the GMC's. With the existence of the oxygen transfer limitation, this structure is able to let the production following the nominal profile by adding an override control scheme in the proposed control strategy.

Acknowledgements

Support for this study from the National Science Council of the Republic of China under the Grant# NSC91-2214-E212-003 is gratefully acknowledged.

References

[1] D. Riesenberg, R. Guthke, High-cell-density cultivation of microorganisms, Appl. Microbiol. Biotechnol. 51 (1999) 422-430.

[2] S.Y. Lee, High cell-density culture of Escherichia coli., Trends Biotechnol. 14 (1996) 98-105.

[3] J.M. Modak, H.C. Lim, Optimal mode of operation of bioreactor for fermentation process, Chem. Eng. Sci. 47 (1992) 3869-3884.

[4] D.J. Korz, U. Rinas, K. Hellmuth, E.A. Sanders, W.-D. Deckwer, Simple fed-batch technique for high cell density cultivation of Escherichia coli., J. Biotechnol. 39 (1995) 59-65.

[5] A. Menawat, R. Mutharasan, D.R. Coughanowr, Singular optimal control strategy for a fed-batch bioreactor: numerical approach, AIChE J. 33 (1987) 776-783.

[6] J. Lee, S.Y. Lee, S. Park, A.P.J. Middelberg, Control of fed-batch fermentations, Biotechnol. Adv. 17 (1999) 29-48.

[7] D. M. Chang, The snowball effect in fed-batch bioreactions, Biotechnol. Prog. 19 (2003) 1064-1070.

[8] J. Bhat, M. Chidambaram, K.P. Madhavan, Robust control of a batch-fed fermenter, J. Proc. Cont. 1 (1991) 146-151.

[9] B. Frahm, P. Lane, H. Atzert, A. Munack, M. Hoffmann, V.C. Hass, R. Pörtner, Adaptive, model-based control by the open-loop-feedback-optimal controller for the effective fed-batch cultivation of hybridoma cells, Biotechnol. Prog. 18 (2002) 1095-1103.

[10] B.S. Kim, S.C. Lee, S.Y. Lee, Production of poly(3-hydroxybutyric acid) by fed-batch culture of Alcaligenes eutrophus with glucose concentration control, Biotechnol. Bioeng. 43 (1994) 892-898.

[11] H. Honda, T. Kobayashi, Fuzzy control of bioprocess, J. Biosci. Bioeng. 89 (2000) 401-408.

[12] J.D. Boškovic, K.S. Narendra, Comparsion of linear, nonlinear and neural-network-based adaptive controllers for a class of fed-batch fermentation process, Automatica 31 (1995) 817-840.

[13] R.D. Gudi, S.L. Shah, M.R. Gray, P.K. Yegneswaran, Adaptive multirate estimation and control of nutrient levels in a fed-batch fermentation using off-line and on-line measurement, Can. J. Chem. Eng. 75 (1997) 562-573.

[14] R.J. Cardello, K.-Y. San, The design of controllers for batch bioreactors, Biotechnol. Bioengng. 32 (1988) 519-526.

[15] J.T. McAvoy, Some results on dynamic interaction analysis of complex control systems, Ind. Eng. Chem. Process Des. Dev. 22 (1983) 42-49.

[16] T. Takagi, M. Sugeno, Fuzzy identification of systems and its applications to modeling and control, IEEE Trans. Syst. Man. Cyber. SMC-15 (1985) 116-132.

[17] Y.-C. Cheng, C.-C. Yu, Nonlinear process control using multiple models: relay feedback approach, Ind. Eng. Chem. Res. 39 (2000) 420-431.

[18] D. E. Riveria, M. Morari, S. Skogestad, Internal model control (4) PID controller design, Ind. Eng. Chem. Res. 25 (1986) 252-265.

[19] P.L. Lee, G.R. Sullivan, Generic model control (GMC), Comput. and Chem. Eng. 12 (1988) 573-580.